Methyl Torsional Interactions in Acetone

Ali G. Ozkabak,[‡] John G. Philis,[†] and Lionel Goodman*

Contribution from Wright and Rieman Chemistry Laboratories, Rutgers, The State University of New Jersey, New Brunswick, New Jersey 08903. *Received April 20, 1990*

Abstract: The ground-state potential surface for methyl torsional interactions in acetone has been obtained by ab initio, semiempirical, and empirical methods. Frequencies acquired from recent Rydberg spectroscopy measurements on the a_2 ground-state fundamental and overtone torsional vibrations and infrared measurements on b_2 fundamentals in acetone-h_6 and acetone-d_6 are well simulated by purely theoretical ab initio HF/6-31G(d,p) and scaled MP2/6-31G(d,p) (i.e., semiempirical) *fully-relaxed* model potentials. This model incorporates skeletal flexing during the methyl rotation, causing the CCC angle to vary by 3°. The single unique empirical surface obtained from the above-mentioned measured frequencies is in good agreement with the ab initio and scaled ones. The four empirically determined constants in the two (equivalent C_{3v}) top potential function, eq 3, are $V_3 = 370$ cm^{-1}, $V_{33} = 136$ cm^{-1}, $V'_{33} = -156$ cm^{-1} and $V_6 = 0$ cm^{-1}. The torsional barrier, V_{eff}, is found to be 240 cm^{-1}, significantly lower than the microwave value. We are unable to predict potential constants that simulate the frequency-generated empirical ones at any level of ab initio calculation [i.e., HF/DZ, HF/6-31G(d,p), and MP2/6-31G(d,p)] within the *rigid-frame* model (i.e., geometry parameters at equilibrium are held fixed during the methyl top rotation).

1. Introduction

The goal of this article is to obtain a physical understanding of the torsional potential interaction in coupled methyl tops. Insight into the potential barrier hindering internal rotations is fundamental to understanding the internal dynamics of flexible molecules. Acetone is our benchmark molecule since it is one of the smallest nonrigid molecules.

Despite its potential as a prototype, acetone has not lived up to a benchmark status because only one methyl torsional vibration is active in infrared and Raman spectra. The a_2 torsional mode fundamental frequency has historically remained unmeasured. Since methyl rotation does not induce appreciable polarizability changes, the a_2 symmetry torsional vibration remains inactive in Raman spectra.[1] This lacuna has prevented calibration of methyl–methyl interaction potential models. Only just recently, two-photon jet spectroscopy involving Rydberg transitions has revealed the missing ground-state a_2 torsional fundamental and its overtone in acetone-h_6 and acetone-d_6.[2]

A comprehensive study by Swalen and Costain[3] carried out over 30 years ago was undertaken to obtain an understanding of the microwave spectrum of acetone. An estimate of the torsional barrier to the methyl rotations was obtained by utilizing rotational splittings resulting from coupling of the two rotational motions, overall and internal, in acetone-h_6 and acetone-d_6. However, Swalen and Costain were forced to assume an effective torsional barrier with no interactions between the two methyl rotors. In this approximation, the two torsional vibration frequencies are equal. Similar microwave studies, carried out more recently by Nelson and Pierce,[4] Peter and Dreizler,[5] and Vacherand et al.,[6] are in very good agreement with the Swalen–Costain rotational constants and torsional barrier estimation.

There have been two notable studies of methyl torsional interactions in acetone. The 1986 study of Crighton and Bell[7] assumed a rigid-frame potential model generated from ab initio ground state energy calculations with use of a modified double-ζ (DZ) basis set. A two-top interaction potential was obtained by methyl rotations against a rigid molecular frame, and electron correlation was not taken into account. The two torsional fundamental frequencies obtained in this study were much higher than the experimental measurements (i.e., 77 ± 2 cm^{-1} for a_2 from the Rydberg spectrum[2] and 124 cm^{-1} for b_2 from infrared studies[8,9]). The 1987 study of Durig and co-workers[10] utilized the acetone-h_6, -d_6, and -d_3 infrared-active torsional vibrational sublevels as observed in the far-infrared spectra. The discrepancies between the three empirically determined potential constants from each labeled molecule spectrum were irreconcilable. Furthermore, these empirical potentials give inaccurate predictions for the a_2–b_2 frequency splittings as revealed by the recent a_2 frequency determinations.[2]

There have been other theoretical studies aimed at obtaining the acetone torsional potential[11] and effective barrier.[12-15] However, these calculations were carried out with inadequate basis sets or without complete geometry optimization of the methyl conformers. The inchoate potential barrier models for acetone have clearly originated in the historical lack of firm experimental observation for the a_2 torsional frequency. The ab initio models were missing a vital calibration point, and the empirical approach had to resort to complex sublevel splittings and difficult to analyze broken symmetry spectra. A secure a_2 torsional frequency allows a systematic assessment of various approaches to the two-top problem. Consequently a purely empirical potential function can be constructed by using the six measured and firmly assigned torsional frequencies in acetone-h_6 and acetone-d_6 [i.e., $\nu_{12}(a_2)$, $\nu_{17}(b_2)$, and $2\nu_{12}$], thus providing a crucial test for theoretical models.

Our main focus is to obtain physical understanding of the coupled methyl top interactions. Although methyl torsional vibration frequencies can be obtained from ab initio harmonic force field calculations, harmonic torsional frequencies obtained in this way are usually not physical, because they are derived from very shallow torsional vibration potentials in the neighborhood of the equilibrium geometry. Thus pointwise determination of the potential is required rather than methods based on the curvature at the minimum.[16] We develop in this paper a theoretical approach for determining accurate torsional potentials for two methyl rotor systems. This involves investigation of the adequacy of the

[‡] Supercomputer Postdoctoral Fellow, 1988-90.
[†] Permanent address: Department of Physics, University of Ioannina, Ioannina, Greece.

(1) Harris, W. C.; Levin, I. W. *J. Mol. Spectrosc.* **1972**, *43*, 117.
(2) Philis, J. G.; Berman, J. M.; Goodman, L. *Chem. Phys. Lett.* **1990**, *167*, 16.
(3) Swalen, J. D.; Costain, C. C. *J. Chem. Phys.* **1959**, *31*, 1562.
(4) Nelson, R.; Pierce, L. *J. Mol. Spectrosc.* **1965**, *18*, 344.
(5) Peter, R.; Dreizler, H. *Z. Naturforsch. Teil* **1965**, *A20*, 301.
(6) Vacherand, J. M.; van Eijck, B. P.; Burie, J.; Demaison, J. *J. Mol. Spectrosc.* **1986**, *118*, 355.
(7) Crighton, J. S.; Bell, S. *J. Mol. Spectrosc.* **1986**, *118*, 383.
(8) Axis choice is shown in Figure 1. References 2 and 7 employ the *z* axis along the C–O bond and *y* axis, out-of-plane, thus switching the b_2 torsional mode symmetry to b_1.
(9) Fateley, W. G.; Miller, F. A. *Spectrochim. Acta* **1962**, *18*, 977. Smith, D. R.; McKenna, B. K.; Möller, K. D. *J. Chem. Phys.* **1966**, *45*, 1904.
(10) Groner, P.; Guirgis, G. A.; Durig, J. R. *J. Chem. Phys.* **1987**, *86*, 565.
(11) Smeyers, Y. G.; Bellido, M. N. *Int. J. Quantum Chem.* **1981**, *19*, 553; **1983**, *23*, 507. Smeyers, Y. G.; Huertas-Cabrera, A. *Theor. Chim. Acta* **1983**, *64*, 97.
(12) Allinger, N. L.; Hickey, M. J. *Tetrahedron* **1972**, *28*, 2157.
(13) Cremer, D.; Binkley, J. S.; Pople, J. A.; Hehre, W. J. *J. Am. Chem. Soc.* **1974**, *96*, 6950.
(14) Bowers, P.; Schäfer, L. *J. Mol. Struct.* **1980**, *69*, 233.
(15) Wiberg, K. B.; Martin, E. *J. Am. Chem. Soc.* **1985**, *107*, 5035.
(16) Lister, D. G.; Macdonald, J. N.; Owen, N. L. *Internal Rotation and Inversion*; Academic: New York, 1978.

0002-7863/90/1512-7854$02.50/0

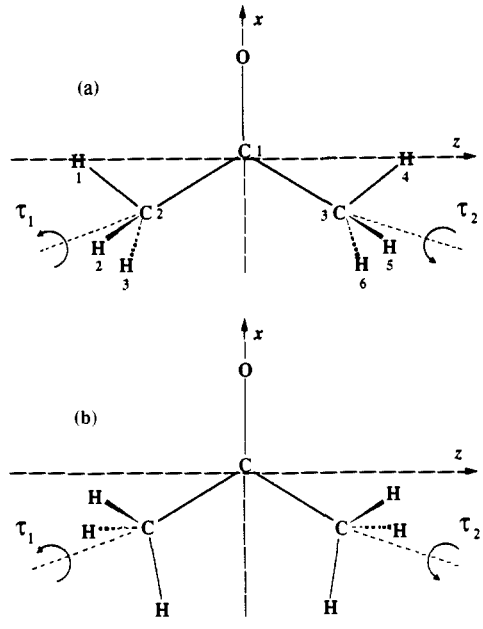

Figure 1. Definitions of two acetone conformers, (a) eclipsed–eclipsed and (b) staggered–staggered, and of internal rotation angles (τ_1, τ_2).

rigid-frame model[7] for describing the methyl top interactions with the molecular frame and with each other. Ab initio calculation of geometric parameters provides a powerful tool for approaching this problem, since it is well established that accurate geometries can be realized by using correlated wave functions constructed from basis sets containing moderate polarization plus diffuse functions.[17] At this level ab initio calculated force constants are, in general, *qualitatively* meaningful and suggest that predicted torsional potential terms will be physical. Another objective is to investigate the efficacy of a semiempirical model obtained by experimental frequency scaling of ab initio calculated potential constants.

2. General Approach

The complete acetone Hamiltonian function was given by Swalen and Costain[3] in 1959. The part relevant to the two internal rotations, including the coupling of the rotors (with rotation angles τ_1 and τ_2), is

$$H = F(p_1^2 + p_2^2) + F'(p_1p_2 + p_2p_1) + V(\tau_1,\tau_2) \quad (1)$$

The first and second terms in eq 1 are kinetic energies of the free and coupled internal rotors, respectively. $p_i = -i(\partial/\partial\tau_i)$ is the generalized momentum, and F and F' are torsional kinetic energy coefficients expressed in terms of the moment of inertia of one methyl rotator about its symmetry axis, I_τ, and the molecular moments of inertia about its principal axes, I_x and I_z. Since the molecular frame is planar (lying in the xz plane of Figure 1), there is no coupling between the methyl rotors and the molecular moment of inertia along the out-of-plane y axis. Thus the torsional kinetic energy coefficients are given as

$$F = \frac{h^2}{4I_\tau}(r_z^{-1} + r_x^{-1}) \quad (2a)$$

$$F' = \frac{h^2}{4I_\tau}(r_z^{-1} - r_x^{-1}) \quad (2b)$$

where

$$r_x = 1 - \frac{2\lambda_x^2 I_\tau}{I_x} \quad (2c)$$

$$r_z = 1 - \frac{2\lambda_z^2 I_\tau}{I_z} \quad (2d)$$

(17) Hehre, W. J.; Radom, L.; Schleyer, P. v. R.; Pople, J. A. *Ab Initio Molecular Orbital Theory*; Wiley: New York, 1986.

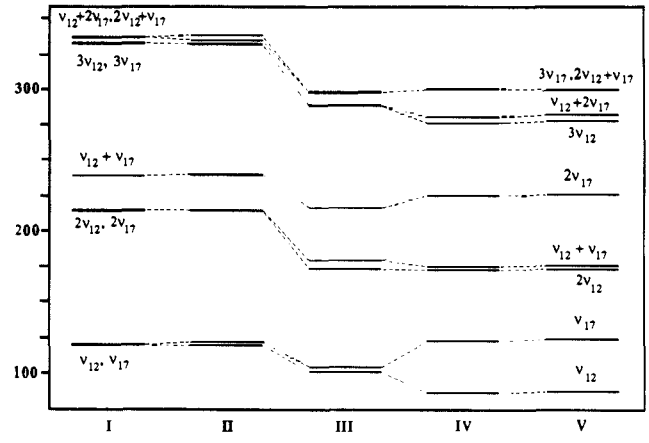

Figure 2. Torsional vibration energy levels for a molecule with two equivalent methyl rotors. Terms in the Hamiltonian (eq 1) are gradually introduced: **I** (F, V_3); **II** (**I**, F'); **III** (**II**, V_{33}); **IV** (**III**, V'_{33}); **V** (**IV**, V_6). The parameter values are $V_3 = 350$ cm^{-1}, $V_{33} = 100$ cm^{-1}, $V'_{33} = -100$ cm^{-1}, $V_6 = -3$ cm^{-1}, $F = 5.7$ cm^{-1}, and $F' = -0.2$ cm^{-1}, chosen for meaningfulness and for effect visibility.

In eqs 2c and 2d, λ_x and λ_z are direction cosines between the methyl top axis and x and z axes, respectively.

The traditional approach[3,18-21] is to expand the potential function, $V(\tau_1,\tau_2)$, written for a C_{2v} molecular frame with two equivalent C_{3v} tops, as a Fourier series in terms of the two rotation angles, τ_1 and τ_2 (defined in Figure 1)

$$V(\tau_1,\tau_2) = \tfrac{1}{2}V_3(\cos 3\tau_1 + \cos 3\tau_2) + \tfrac{1}{2}V_{33}(\cos 3\tau_1 \cos 3\tau_2) + \tfrac{1}{2}V'_{33}(\sin 3\tau_1 \sin 3\tau_2) + \tfrac{1}{2}V_6(\cos 6\tau_1 + \cos 6\tau_2) + \ldots \quad (3)$$

Since the constant term in the potential function in eq 3 has been eliminated for convenience, the torsional energy levels are obtained relative to the lowest level. Terms of higher order than V_6 are also traditionally dropped. The three cosine terms in eq 3 describe interactions of methyl rotors with the frame and with each other leaving the two torsional fundamental frequencies equal. This degeneracy, however, is lifted by introducing the sine term, V'_{33}, which describes methyl–methyl interactions. The degeneracy of the torsional fundamental vibration energies is also lifted by the kinetic coupling term, F', in the Hamiltonian. The Hamiltonian in eq 1 neglects interaction between torsions and the other vibrations.

The effects of the four potential constants (V_3, V_{33}, V'_{33}, V_6) and the two torsional kinetic energy coefficients (F and F') on the torsional vibrational energies are illustrated in Figure 2. A physically meaningful set of parameter magnitudes ($V_3 = 350$ cm^{-1}, $V_{33} = 100$ cm^{-1}, $V'_{33} = -100$ cm^{-1}, $V_6 = -3$ cm^{-1}, $F = 5.7$ cm^{-1}, and $F' = -0.2$ cm^{-1}) has been chosen. Only V_3 and F are included in example I. At this level the a_2 and b_2 torsional fundamentals (ν_{12} and ν_{17}, respectively) and their harmonics are degenerate. The combination bands (e.g., $\nu_{12} + \nu_{17}$) are not degenerate with the corresponding harmonics, however. II shows that the only effect of F' is to slightly split the degeneracies. III demonstrates the strong perturbing effect of the V_{33} term on the average frequencies of the torsional fundamentals. It also shows that V_{33} has no effect on the fundamental splittings (the effect on overtone and combination level splittings is substantial). IV clearly reveals that the potential term mainly responsible for the splitting between the a_2 and b_2 torsional fundamentals is V'_{33}. V demonstrates that V_6 only produces minor perturbations on frequencies and splittings. Thus calibration of the important V'_{33} term can be quite accurately obtained from the observed splitting between the two torsional fundamental frequencies. The difference $V_3 - V_{33}$ is obtainable from the average of the two frequencies (it is for this reason that $V_3 - V_{33}$ is usually defined as V_{eff}).

(18) Myers, R. J.; Wilson, E. B., Jr. *J. Chem. Phys.* **1960**, *33*, 186.
(19) Möller, K. D.; Andresen, H. G. *J. Chem. Phys.* **1962**, *37*, 1800.
(20) Grant, D. M.; Pugmire, R. J.; Livingston, R. C.; Strong, K. A.; McMurry, H. L.; Brugger, R. M. *J. Chem. Phys.* **1970**, *52*, 4424.
(21) Groner, P.; Durig, J. R. *J. Chem. Phys.* **1977**, *66*, 1856.

Although there is a substantial literature of two-top interactions, the majority of studies are particularly aimed at microwave spectral interpretations. In such studies, the torsional potential is introduced as a perturbation to overall rotation, hence knowledge of a so-called *effective potential*, V_{eff}, usually suffices. However, the effective potential is incapable of uniquely describing the resulting torsional vibrations since they are produced with equal frequencies. In order to understand internal rotations in coupled top systems, the details of the potential function are requisite.

The torsional eigenvalue equation, $H\varphi = E\varphi$, can now be written and its solutions are desired. In order to obtain these solutions, it is convenient to transform the Hamiltonian by introducing[18]

$$\tau_+ = \tfrac{1}{2}(\tau_1 + \tau_2),\ \tau_- = \tfrac{1}{2}(\tau_1 - \tau_2)$$
$$p_+ = (p_1 + p_2),\ p_- = (p_1 - p_2) \quad (4)$$

hence

$$H = \tfrac{1}{2}(F + F')p_+^2 + \tfrac{1}{2}(F - F')p_-^2 + V_3 \cos 3\tau_+ \cos 3\tau_- + \tfrac{1}{4}(V_3 - V'_{33}) \cos 6\tau_+ + \tfrac{1}{4}(V_3 + V'_{33}) \cos 6\tau_- + V_6 \cos 6\tau_+ \cos 6\tau_- \quad (5)$$

Solutions of the Schrödinger equation for the two-top torsional vibraion problem can be obtained by using a product of free internal rotor functions,[22] $\exp[i(3v_+ + \sigma_+)\tau_+] \exp[i(3v_- + \sigma_-)\tau_-]$, as a basis function. Each function is characterized by the two parameters v and σ, where $v = 0, \pm1, \pm2, \ldots$ is related to the vibrational quantum number and $\sigma = 0, 1$ describes the degeneracy of the energy levels.

The Hamiltonian matrix in this basis is separated into four submatrices with (a) $\sigma_+ = 0$, $\sigma_- = 0$ for nondegenerate A levels, (b) $\sigma_+ = 0$, $\sigma_- = 1$ and $\sigma_+ = 1$, $\sigma_- = 0$ for two doubly degenerate E levels, and (c) $\sigma_+ = 1$, $\sigma_- = 1$ for quadruply degenerate Q levels. In the high-barrier limit, these nine sublevels coalesce into a 9-fold degenerate torsional level. In the finite barrier case, partial splitting of this degeneracy results from the tunneling between the three minima of each methyl group.

The Hamiltonian matrix elements have been explicitly given by Crighton and Bell as[7]

$$\langle m_+,m_-|H|m_+,m_-\rangle = \tfrac{1}{2}(F + F')\, m_+^2 + \tfrac{1}{2}(F - F')m_-^2 \quad (6a)$$
$$\langle m_+,m_-|H|m_+ \pm 3,\ m_- \pm 3\rangle = \tfrac{1}{4}\, V_3 \quad (6b)$$
$$\langle m_+,m_-|H|m_+ \pm 3,\ m_- \mp 3\rangle = \tfrac{1}{4}V_3 \quad (6c)$$
$$\langle m_+,m_-|H|m_+ \pm 6,\ m_-\rangle = \tfrac{1}{8}(V_{33} - V'_{33}) \quad (6d)$$
$$\langle m_+,m_-|H|m_+,m_- \pm 6\rangle = \tfrac{1}{8}(V_{33} + V'_{33}) \quad (6e)$$
$$\langle m_+,m_-|H|m_+ \pm 6,\ m_- \pm 6\rangle = \tfrac{1}{4}V_6 \quad (6f)$$
$$\langle m_+,m_-|H|m_+ \pm 6,\ m_- \mp 6\rangle = \tfrac{1}{4}V_6 \quad (6g)$$

where $m_\pm = 3v_\pm + \sigma_\pm$. Substitutions given in eq 4 impose restrictions on the allowable m_+ and m_- values in each basis function; i.e., they are either both even or both odd. Although the basis set contains an infinite number of functions, it is sufficient to consider the range $-10 \le v_\pm \le +10$ for convergence of the first ten acetone-h_6 and -d_6 torsional levels. The torsional energy levels are finally obtained by diagonalization of the Hamiltonian submatrices.

3. Ab Initio Calculations

Ab initio Hartree-Fock (HF) calculations were carried out with the Huzinaga-Dunning double-ζ (DZ)[23] and the Pople 6-31G(d,p),[24] basis sets in order to examine the effect of polarization functions on the predicted acetone internal rotations. In addition, electron correlation effects were obtained by second-order Møller-Plesset (MP2) theory with the 6-31G(d,p) basis set. The computations were performed with use of the GAUSSIAN 88 program[25] on a Cray Y-MP. Default geometry optimization thresholds have been utilized: 4.5×10^{-4} hartree/bohr or hartree/rad for maximum internal coordinate force, and 3×10^{-4} hartree/bohr or hartree/rad for the root-mean-square force. These criteria lead to $<10^{-3}$ mydn for typical residual Cartesian forces on a given atom.

Potential energy calculations were carried out at two levels. The first involved rotation of methyl groups from the most stable equilibrium positions without alterations of the molecular frame or the relative hydrogen atom orientations in the two methyl tops. This geometry invariance to internal rotations is termed the *rigid-frame model*. The second involved complete geometry optimization for each of the methyl conformers (i.e., *fully-relaxed model*). Initially, geometry optimization was carried out with eight parameters constraining one hydrogen atom in each methyl group to lie in the plane of the molecular frame, but allowing nonequivalent CH bond lengths and HCH bond angles for the in- and out-of-plane hydrogen atoms. The two methyl groups were situated so that the molecule conformed to C_{2v} symmetry. The eclipsed-eclipsed equilibrium geometry (i.e., in-plane hydrogen atoms in both methyl tops eclipsed by oxygen) shown in Figure 1a was found. In the rigid-frame model, the equilibrium geometry parameters were retained during the methyl rotations. In contrast, the fully-relaxed model potentials were obtained by optimizing with additional parameters for the non-C_{2v} conformers (see Table IX). For example, the least symmetric conformer required 21 independent parameters to be optimized (i.e., molecular frame planarity and the two torsional angles, τ_1 and τ_2, defining the conformer were excluded from the 24 degrees of freedom).

3.1. Geometry. The predicted ground-state equilibrium geometries of acetone obtained from ab initio calculations (i.e., r_e structures) are summarized in Table I. All basis sets predict the eclipsed-eclipsed structure (Figure 1a) to be the most stable nuclear configuration. Moreover, the eclipsed structure in-plane CH bonds are always ~0.005 Å shorter than the out-of-plane CH bonds. The CO and CH bond distances are particularly sensitive to polarization functions in the basis set and electron correlation. Table I also shows the methyl staggered (Figure 1b) acetone optimized geometry parameters from the ab initio calculations. The differences between the staggered and eclipsed conformers are mainly in the bond angles (i.e., 2-3° changes) and in the CC bond length (i.e., 0.004-Å changes). The CH bond lengths are almost the same for these two methyl conformers.

The experimental ground-state geometry of acetone, determined from microwave spectra (r_s structure) by Nelson and Pierce,[4] and the geometry determined from combined microwave and gas electron diffraction data (r_z/r_e structure) by Iijima[26] are also given in Table I. These two experimental determinations differ substantially from one another, particularly for the CC bond distance and the CCC bond angle.

The most important difference between the two experimental geometries and those obtained from the ab initio calculations is the nonequivalence of the CH bond distances in each methyl top. The ~0.005-Å difference between CH_{ip} and CH_{op}, although consistently predicted by the ab initio calculations, was not detected by an electron diffraction analysis that specifically sought this difference.[27] It appears probable that microwave data would not detect it either. Thus a tilt angle of approximately 2° between the methyl top axis and the CC bond that has been invoked[4,26] to reproduce the observed acetone rotational constants may actually be compensating for unequal CH distances.

A more meaningful comparison can be made between the moments of inertia obtained for acetone-h_6 and -d_6 from the experimental and calculated geometries. Ultimately moments of inertia are microwave observables rather than bond lengths or bond angles. The discrepancies between the two experimental moments are less than 1 amu Å^2, suggesting that the differences in the experimental bond lengths and bond angles[4,26] might result from different interpretations. The most important conclusion is that, as Table I clearly shows, there is a very good agreement between the experimental and calculated *eclipsed* structure moments of inertia. In the staggered structures, an additional stability is attained by readjusting the bond lengths and bond angles, and consequently, the calculated staggered and eclipsed conformer moments differ by as much as 3.2 amu Å^2.

The torsional kinetic energy coefficients, F and F' (eqs 2a-d), depend on the atomic masses and geometry parameters and are also presented in Table I. These coefficients enter the diagonal Hamiltonian matrix elements (eq 6a) and have profound effects on the torsional energy levels.

(22) Herschbach, D. R. *J. Chem. Phys.* **1959**, *31*, 91.
(23) Huzinaga, S. *J. Chem. Phys.* **1965**, *42*, 1293. Dunning, T. H. *J. Chem. Phys.* **1970**, *53*, 2823.
(24) Hariharan, P, C.; Pople, J. A. *Theor. Chim. Acta* **1973**, *28*, 213.
(25) Frisch, M. J.; Head-Gordon, M.; Schlegel, H. B.; Raghavachari, K.; Binkley, J. S.; Gonzalez, C.; Defrees, D. J.; Fox, D. J.; Whiteside, R. A.; Seeger, R.; Melius, C. F.; Baker, J.; Martin, R. L.; Kahn, L. R.: Steward, J. J. P.; Fluder, E. M.; Topiol, S.; Pople, J. A. GAUSSIAN 88, Gaussian, Inc.: Pittsburgh, PA, 1988.
(26) Iijima, T. *Bull. Chem. Soc. Jpn.* **1972**, *45*, 3526.
(27) Klimkowski, V. J.; Pulay, P.; Ewbank, J. D.: McKean, D. C.; Schäfer, L. *J. Comp. Chem.* **1984**, *5*, 517.

Table I. Experimental and ab Initio Optimized Geometries and Acetone-h_6 and -d_6 Moments of Inertia and Torsional Kinetic Energy Coefficients[a]

	MW,[b]	MW & GED[c]	HF/DZ		HF/6-31G(d,p)		MP2/6-31G(d,p)	
	ee	ee	ee	ss	ee	ss	ee	ss
bond lengths								
C-O	1.222	1.210	1.2245	1.2257	1.1923	1.1928	1.2257	1.2256
C-C	1.507	1.517	1.5132	1.5174	1.5130	1.5172	1.5112	1.5159
$C-H_{ip}$	1.085	1.083	1.0795	1.0798	1.0810	1.0823	1.0847	1.0853
$C-H_{op}$	1.085	1.083	1.0846	1.0835	1.0863	1.0845	1.0892	1.0879
bond angles								
C-C-C	117.2	115.0	117.3	119.8	116.7	119.6	116.4	119.4
$C-C-H_{ip}$	108.8	107.8	110.1	112.7	109.7	113.3	109.6	113.2
$C-C-H_{op}$	110.8	110.8	110.2	109.3	110.3	108.7	110.2	108.8
$H_{ip}-C-H_{op}$	108.8	109.1	109.4	109.1	109.6	109.2	109.8	109.4
$H_{op}-C-H_{op}$	108.8	109.1	107.5	107.1	107.2	107.4	107.2	107.3
moments of inertia								
acetone-h_6								
I_z	49.422872	50.220457	49.687750	48.381683	48.674746	47.136191	50.225842	48.554072
I_x	59.299334	58.637605	59.632555	61.589459	59.241874	61.440718	58.939476	61.314842
I_y	102.446858	102.582559	103.154514	103.844266	101.750294	102.419125	102.965058	103.677460
I_τ	3.137605	3.137730	3.121199	3.107708	3.134245	3.122669	3.156715	3.143019
F	5.728337	5.723396	5.749745	5.791311	5.733357	5.776021	5.686391	5.730736
F'	−0.208666	−0.198535	−0.178061	−0.256323	−0.179613	−0.270837	−0.168112	−0.259802
F_{av}			5.770528		5.754689		5.708564	
F'_{av}			−0.217192		−0.225225		−0.213957	
acetone-d_6								
I_z	59.166679	60.047077	59.489301	57.904083	58.451703	56.609097	60.141349	58.145122
I_x	78.858853	77.959169	79.151434	81.800886	78.639893	81.603402	78.268183	81.470192
I_y	125.484489	125.464890	126.318636	127.460639	124.768427	125.906402	126.018548	127.241929
I_τ	6.270384	6.270635	6.237598	6.210636	6.263670	6.240535	6.308575	6.281204
F	2.997929	2.993125	3.003283	3.038410	2.996684	3.035231	2.969883	3.008660
F'	−0.197472	−0.188564	−0.170026	−0.240008	−0.171145	−0.252761	−0.161341	−0.243169
F_{av}			3.020847		3.015958		2.989272	
F'_{av}			−0.205017		−0.211953		−0.202255	

[a] Bond lengths and bond angles are in Å and deg, respectively. Moments of inertia are in amu Å^2. Torsional kinetic energy coefficients, F and F', are in cm^{-1}. ee and ss denote eclipsed-eclipsed and staggered-staggered, respectively. [b] Microwave (MW) geometry is from ref 4. [c] Combined microwave (MW) and gas electron diffraction (GED) geometry is from ref 26.

Table II. Acetone Methyl Conformer Energies Relative to Eclipsed-Eclipsed Conformer[a]

conformer		HF/DZ		HF/6-31G(d,p)		MP2/6-31G(d,p)	
τ_1, deg	τ_2, deg	rigid-frame	fully-relaxed	rigid-frame	fully-relaxed	rigid-frame	fully-relaxed
60	60	0[b]	0[b]	0[c]	0[c]	0[d]	0[d]
0	60	282.78	238.16	340.56	246.85	351.58	267.07
0	0	970.57	785.24	1079.04	763.92	1086.83	793.62
30	60	193.74	114.16	228.94	120.82	232.70	129.31
0	30	679.40	513.69	761.61	508.94	774.73	535.53
30	30	385.14	221.84	447.94	229.71	461.45	252.34

[a] Full optimization for each conformer is obtained by as many as 21 parameter optimizations depending on the conformer symmetry. Rigid-frame calculations are carried out by rotating the methyl groups from the eclipsed-eclipsed conformer ($\tau_1 = \tau_2 = 60°$) without adjusting the geometry. Relative energies are in cm^{-1}. [b] Total HF/DZ energy is −191.905 857 hartrees. [c] Total HF/6-31G(d,p) energy is −191.972 072 hartrees. [d] Total MP2/6-31G(d,p) energy is −192.589 477 hartrees.

There is a very good agreement between the F coefficients of acetone-h_6 and acetone-d_6 obtained from the two experimental geometries, and the F' coefficients differ by only 0.01 cm^{-1}.

The coefficients obtained from the theoretical geometries show fair agreement with the values derived from the experimental geometries. This agreement for the ab initio F values is better than that for the ab initio F' values. The former are insensitive to methyl orientations, for the latter eclipsed geometries produce 0.03–0.04 cm^{-1} smaller magnitudes than the experimental ones and staggered geometries give 0.06–0.07 cm^{-1} higher magnitudes. In retrospect, the fully-relaxed ab initio model suggests that the kinetic energy coefficients F and F' reach these two extremes during the methyl rotations. It appears reasonable to assume that effective kinetic energy coefficients represent an average of the eclipsed and staggered extreme values. The averaged kinetic energy coefficients given in Table I are now in very good agreement with the experimental values for both F and F'. These kinetic energy coefficient averages were used for the fully-relaxed model torsional energy calculations (vide infra). For the rigid-frame model, eclipsed values were utilized consistent with the predicted geometry.

3.2. Conformer Energies and Potential Constants. In order to determine the torsional potential function in the form of eq 3, we calculated the total molecular energies at discrete methyl rotation angles, τ_1 and τ_2 (i.e., methyl conformers). Since the internal rotation potential is expanded into a four-term function, at least five symmetrically nonequivalent conformers are required for its determination. (One conformer is needed to fix the potential minimum.)

The torsional potential function in eq 3 engenders two approximations: (a) methyl tops rotate around the C_3 axes and (b) terms beyond V_6 are negligible. The errors resulting from these approximations can be assessed by generating more than the required minimum number of conformer energies. Hence, we have carried out ab initio calculations for six methyl conformers. The methyl conformers were defined as repositioning the in-plane hydrogen atoms with respect to the molecular frame, so that the hydrogen atom dihedral angles are changed by $3\tau_1$ and $3\tau_2$ from the eclipsed equilibrium geometry. Then the energy calculations were carried out in accordance with the two models (i.e., rigid-frame and fully-relaxed).

These six conformers are the following: (1) $\tau_1 = 60°$, $\tau_2 = 60°$ (eclipsed-eclipsed); (2) $\tau_1 = 0°$, $\tau_2 = 0°$ (staggered-staggered); (3) $\tau_1 = 0°$, $\tau_2 = 60°$; (4) $\tau_1 = 30°$, $\tau_2 = 60°$; (5) $\tau_1 = 0°$, $\tau_2 = 30°$; and (6) $\tau_1 = 30°$, $\tau_2 = 30°$. The conformer energies for the rigid-frame and fully-relaxed models are given in Table II. The HF/DZ rigid-frame model produces a 971-cm^{-1} barrier for the methyl rotations (i.e., staggered-staggered conformer energy relative to the eclipsed-eclipsed conformer). This barrier, 1080 cm^{-1} with the polarization function containing the 6-31G(d,p) basis set, remains almost unaffected by electron correlation. There is a similar 10–20% increase in energy of the other conformers when polarization functions are included in the basis set and less than 3% when electron correlation is included.

The fully-relaxed model conformer energies are found to be 30–45% smaller than the rigid-frame ones and consequently the torsional barrier height is greatly lowered, by nearly 300 cm^{-1}. The correlation corrections

Table III. Ab Initio Calculated Potential Energy Constants for Internal Rotations in Acetone[a]

method	V_3	V_{33}	V'_{33}	V_6	V_{eff}[b]
rigid-frame					
HF/DZ	485.29	202.51	-207.94	-52.54	282.78
HF/6-31G(d,p)	539.52	198.96	-205.16	-55.24	340.56
MP2/6-31G(d,p)	543.42	191.84	-196.98	-56.22	-351.58
fully-relaxed					
HF/DZ	392.62	154.46	-181.26	1.46	238.16
HF/6-31G(d,p)	381.96	135.11	-171.28	-0.47	246.85
MP2/6-31G(d,p)	396.81	129.74	-161.12	-0.48	267.07

[a] Internal rotation potential energy is expressed as $2V(\tau_1,\tau_2) = V_3(\cos 3\tau_1 + \cos 3\tau_2) + V_{33}\cos 3\tau_1 \cos 3\tau_2 + V'_{33}\sin 3\tau_1 \sin 3\tau_2 + V_6(\cos 6\tau_1 + \cos 6\tau_2)$. Potential constants are in cm^{-1}. [b] Effective rotation barrier, $V_{eff} = V_3 - V_{33}$, is the change in potential energy obtained by rotating one methyl group through 60° from its equilibrium position.

Table IV. Calculated Torsional Energy Levels and Maximum Splittings Caused by Tunneling for Acetone-h_6 and -d_6 Using the Fully-Relaxed HF/6-31G(d,p) Potential[a]

level no.	A	E_1	E_3	Q	Δ[b]
		Acetone-h_6[c]			
1	0.00	0.17	0.17	0.09	0.17
2	79.54	78.17	78.16	78.83	1.38
3	130.41	127.07	127.07	128.74	3.34
4	163.85	170.45	170.73	165.86	6.88
5	174.36	188.16	187.56	182.26	13.80
6	234.67	230.94	233.27	232.81	3.73
7	270.06	244.51	241.43	251.15	28.63
8	282.34	257.92	259.07	274.06	24.42
9	303.83	290.07	290.04	301.64	13.79
10	309.83	336.53	336.61	308.84	27.77
		Acetone-d_6[d]			
1	0.00	0.01	0.01	0.00	0.01
2	54.70	54.64	54.64	54.67	0.06
3	99.12	98.93	98.93	99.03	0.19
4	117.85	118.29	118.29	118.06	0.44
5	141.01	142.48	142.47	141.74	1.47
6	185.60	182.13	182.47	183.48	3.47
7	188.80	191.42	189.09	190.06	2.62
8	198.69	191.74	193.92	195.35	6.95
9	227.59	217.89	217.59	222.56	10.00
10	231.47	247.36	246.40	232.68	15.89

[a] Energies are in cm^{-1}. Kinetic energy coefficients; acetone-h_6, F = 5.754689 cm^{-1}, F' = -0.225225 cm^{-1}; acetone-d_6, F = 3.015958 cm^{-1}, F' = -0.211953 cm^{-1}. Potential energy parameters: V_3 = 381.97 cm^{-1}, V_{33} = 135.11 cm^{-1}, V'_{33} = -171.28 cm^{-1}, V_6 = -0.47 cm^{-1}. [b] Maximum splitting between the A, E_1, E_3, and Q levels in cm^{-1}. [c] Zero-point energy = 107.00 cm^{-1}. [d] Zero-point energy = 78.13 cm^{-1}.

are much more significant in the fully-relaxed model potential compared to those in the rigid-frame model.

The relative conformer energies given in Table II are fitted to the acetone torsional potential (eq 3), allowing the four constants, V_3, V_{33}, V'_{33}, and V_6, to be obtained (Table III). In all cases, only two conformer energies (τ_1 = 30°, τ_2 = 60° and τ_1 = 0°, τ_2 = 30°) deviate from the fitted surfaces, and these by less than 5 cm^{-1}. Hence, despite predicted asymmetry in the methyl conformations, the four-term potential (eq 3) conforming to C_3 symmetry is suitable for acetone internal rotations.

The four potential parameters obtained from the HF and MP2 calculations show striking differences between the rigid-frame and fully-optimized models. This is particularly so for the V_3 and V_6 terms. The V_3 term is predicted to be ~500 and ~400 cm^{-1}, in the rigid-frame and fully-relaxed potentials, respectively. The V_6 term is drastically reduced from -55 cm^{-1} in the rigid-frame model to ~0 by optimizing each methyl conformer. The effect of polarization function inclusion in the basis set is only appreciable on V_3 in the rigid-frame model, but it causes all four potential parameter magnitudes to be considerably lowered in the fully-relaxed model.

A physical understanding of the rigid-frame potentials can be obtained by examining the magnitudes of the cosine and sine coupling terms, V_{33} and V'_{33}, which are almost equal with opposite signs. This is interpreted as gearing of the two methyl tops causing the tops to rotate freely for certain phases (i.e., $\tau_1 + \tau_2$ = 60°, 180°, etc.). However, in the fully-relaxed model there is a considerable disparity between the magnitudes of the cosine and the sine coupling terms at every level of calculation. Consequently, gearing in acetone is predicted to be less effective than is concluded from the simple rigid-frame picture.[7]

Table V. Calculated Torsional Energy Levels and Maximum Splittings Caused by Tunneling for Acetone-h_6 and -d_6 Using the Rigid-Frame HF/6-31G(d,p) Potential[a]

level no.	A	E_1	E_3	Q	Δ[b]
		Acetone-h_6[c]			
1	0.00	0.03	0.03	0.02	0.03
2	118.48	117.97	117.97	118.23	0.51
3	169.18	167.99	167.99	168.58	1.19
4	227.80	233.24	233.31	229.72	5.51
5	239.47	248.96	248.81	244.90	9.49
6	309.91	300.68	302.26	302.74	9.23
7	344.51	307.85	306.03	319.99	38.48
8	348.22	328.18	328.54	346.27	20.04
9	361.53	384.82	384.55	368.11	23.29
10	373.41	415.20	416.24	389.62	42.83
		Acetone-d_6[d]			
1	0.00	0.00	0.00	0.00	0.00
2	87.35	87.34	87.34	87.34	0.01
3	130.70	130.67	130.67	130.69	0.03
4	174.04	174.21	174.21	174.13	0.17
5	197.43	197.92	197.92	197.68	0.49
6	251.72	252.16	252.51	252.06	0.79
7	256.75	254.41	253.90	255.06	2.85
8	265.24	260.49	260.67	263.21	4.75
9	302.87	297.89	297.77	300.92	5.10
10	304.31	318.17	318.55	303.60	14.95

[a] Energies are in cm^{-1}. Kinetic energy coefficients: acetone-h_6, F = 5.733357 cm^{-1}, F' = -0.179613 cm^{-1}; acetone-d_6, F = 2.996684 cm^{-1}, F' = -0.171145 cm^{-1}. Potential energy parameters: V_3 = 539.52 cm^{-1}, V_{33} = 198.96 cm^{-1}, V'_{33} = -205.16 cm^{-1}, V_6 = -55.24 cm^{-1}. [b] Maximum splitting between the A, E_1, E_3, and Q levels in cm^{-1}. [c] Zero-point energy = 156.56 cm^{-1}. [d] Zero-point energy = 115.65 cm^{-1}.

Table VI. Experimental and Predicted Torsional Fundamental Frequencies in Acetone-h_6 and -d_6[a]

	acetone-h_6		acetone-d_6	
method	$\nu_{12}(a_2)$	$\nu_{17}(b_2)$	$\nu_{12}(a_2)$	$\nu_{17}(b_2)$
experimental[b]	77 ± 2	124.5 ± 0.1	55 ± 2	96.0 ± 0.1
rigid-frame				
HF/DZ	105.7 ± 0.5	157.0 ± 1.2	78.2	123.0
HF/6-31G(d,p)	118.2 ± 0.3	168.4 ± 0.6	87.3	130.7
MP2/6-31G(d,p)	121.1 ± 0.2	169.1 ± 0.5	89.6	130.9
fully-relaxed				
HF/DZ	75.8 ± 0.7	127.7 ± 1.8	52.0	98.3 ± 0.1
HF/6-31G(d,p)	78.7 ± 0.7	128.3 ± 1.7	54.7	99.0 ± 0.1
MP2/6-31G(d,p)	84.0 ± 0.6	130.6 ± 1.3	59.0	100.4 ± 0.1

[a] Frequencies are in cm^{-1}. Predicted frequencies are averages of torsional sublevel energies with half-maximum splittings as their band half-widths (indicated if ≥0.1 cm^{-1}). [b] a_2 and b_2 observed fundamental frequencies are from refs 2 and 10, respectively.

3.3. Torsional Energy Levels. We now turn to the torsional energy levels calculated by the two model potentials. Ultimately the test of the two models resides in the energy levels. The ground-state acetone-h_6 and -d_6 torsional energy levels have been calculated by diagonalizing the Hamiltonian (eq 5) with use of the ab initio potential energy constants and kinetic energy coefficients determined from the rigid-frame and fully-relaxed models. We have tested the effect of using a finite basis set and find $|\nu_\pm|_{max}$ = 10 to be sufficient for ±0.01 cm^{-1} accuracy in the first ten torsional levels.

Since the acetone torsional barrier is finite, splitting of each torsional level is anticipated, leading to separate diagonalization of Hamiltonian submatrices corresponding to the A, E_1, E_3, and Q levels.[18,20] The first ten torsional sublevels and splittings in acetone-h_6 and -d_6 obtained from the fully-relaxed and rigid-frame HF/6-31G(d,p) potentials are given in Tables IV and V, respectively. The effect of tunneling on the second and third torsional levels is important to our analysis, since these levels represent the a_2 and b_2 vibrational fundamentals. The splittings of the second and third levels are between 1 and 3 cm^{-1} in acetone-h_6 and less than 0.2 cm^{-1} in acetone-d_6. However, the higher order torsional levels (i.e., levels 7–10) split by as much as 40 cm^{-1}.

Torsional vibrational frequencies obtained from the rigid-frame and fully-relaxed model potentials are summarized in Table VI (see section 4 for relating torsional energies to vibrational frequencies). There is a marked difference between predicted frequencies by the two models. The rigid-frame model predicts the a_2 and b_2 torsional fundamental frequencies to be ~30–45 and ~25–35 cm^{-1} higher than the experimental values for acetone-h_6 and -d_6, respectively. Both of these frequencies

show an increase of ~10–15 cm^{-1} upon polarization function inclusion in the basis set. The effect of electron correlation is much smaller, increasing the a_2 frequency by 3 cm^{-1}, with almost no change in the b_2 frequency.

In contrast, both torsional fundamental frequencies obtained from the fully-relaxed model potentials are in very good aggreement with experiment. Despite the good predictions, there are subtle differences between the fundamental frequencies calculated by using different potentials reflecting the effect of polarization functions and electron correlation inclusion. The HF level potentials [i.e., HF/DZ and HF/6-31G(d,p)] give <3 cm^{-1} discrepancy for the a_2 frequency and <4 cm^{-1} for the b_2 frequency in acetone-h_6 and -d_6. Although, the fully-relaxed MP2/6-31G(d,p) potential predicts poorer frequencies than the HF potentials, there is an error consistency. For acetone-h_6, the MP2 predicted fundamental frequencies are 7 cm^{-1} higher than the experimental frequencies for both torsional vibrations, and 4 cm^{-1} in the case of acetone-d_6.

4. Discussion

In order to relate predicted torsional level energies to experimental torsional frequencies, it is necessary to examine the level splittings resulting from tunneling. Since it is not always possible to resolve torsional sublevels in the spectrum or to carry out complete rovibrational analyses for these torsional bands, we incorporate the level splittings into the torsional energies. Only the upper level splitting is considered for transitions from the lowest torsional energy level, since the zero-point splitting is negligible. The predicted torsional frequencies reported in this study are comprised of the average energies of the sublevels with half of the corresponding maximum splitting as their calculated band half-widths. As seen in Table IV for the fully-relaxed HF/6-31G(d,p) potential model predictions, this procedure seems reasonable for torsional levels 1–4 and 6 in acetone-h_6 and levels 1–8 in acetone-d_6. The transition to the fifth level in acetone-h_6 (maximum splitting: 14 cm^{-1}) is predicted to appear in the spectrum (if all lines are active) as a triplet with ~7 cm^{-1} component separations. The first three levels are the main focus in our study since they are involved in the two torsional fundamental transition bands. In addition, levels 4–6 are involved in the overtone and torsional combination bands, for which some infrared and Rydberg data are available. Sequence transition analyses are considerably more complex, since the splittings in both initial and final states must be taken into account.

Two bands were reported in the torsional fundamental region of the far-infrared spectrum of acetone-h_6.[9,10] The 124.5-cm^{-1} band is securely attributed to the b_2 fundamental, ν_{17}, while the assignment of the second band at a frequency of 104.5 cm^{-1} is uncertain.[28] In acetone-d_6, the infrared active fundamental is observed[10] at 96.0 cm^{-1}. Our Rydberg experiments[2] established the a_2 torsional fundamental, ν_{12}, frequencies in acetone-h_6 and -d_6. These are 77 ± 2 and 55 ± 2 cm^{-1} in acetone-h_6 and -d_6, respectively. Also determined from the Rydberg spectra are $2\nu_{12}$ overtone frequencies: 162 ± 4 and 117 ± 2 cm^{-1} in acetone-h_6 and -d_6, respectively.[29] These overtone frequencies are useful as further probes of the torsional potential surface.

As pointed out in section 3.3, there are large differences between torsional potential surfaces predicted by the rigid-frame and fully-relaxed models at any ab initio calculation level that we have attempted. The predicted fundamental frequencies for the acetone-h_6 torsional vibrations (Table VI) 78.7 ± 0.7 (a_2) and 128.3 ± 1.7 cm^{-1} (b_2) by the HF/6-31G(d,p) fully-relaxed model are in good agreement with experiment. In contrast the rigid-frame model at the same level of calculation [i.e., HF/6-31G(d,p)] predicts frequencies for the two fundamentals >40 cm^{-1} too high. This large disparity exists for all levels of rigid-frame model calculations in our study. For acetone-d_6, the fundamental frequencies are equally well predicted by the fully-relaxed model and poorly so by the rigid-frame model at the HF/6-31G(d,p) level. The predicted first overtone frequencies for the a_2 torsions 167.7 ± 3.4 and 118.1 ± 0.2 cm^{-1} in acetone-h_6 and -d_6 by the HF/6-31G(d,p) fully-relaxed potential are also in good agreement with experiment. Rigid-frame calculations for the overtones are in gross disparity as is the case for the fundamentals.

Another approach is to obtain the torsional potential by scaling. Such scaling is analogous to ab initio harmonic force constant scaling to fit experimental vibrational frequencies which, for example, Pulay has successfully applied to benzene vibrations.[30] The MP2/6-31G(d,p) fully-relaxed model frequency predictions are approximately equally higher than the experimental ones for both fundamentals. Thus this potential function seems appropriate for scaling. The scaling factor, 0.88, was found to be optimal to give the best overall agreement between predicted and experimental frequencies (Table VII). The a_2 torsional vibration overtone frequencies in acetone-h_6 and -h_6 are also predicted to be in excellent agreement with experiment (Table VIII).

It is possible to generate a purely empirical torsional potential function from the knowledge of the two torsional fundamental, ν_{12} and ν_{17}, and overtone, $2\nu_{12}$, frequencies measured for both acetone-h_6 and -d_6. We have used a three-constant potential, neglecting the V_6 term in eq 3, since its magnitude is almost zero in the theoretical fully-relaxed model potentials. The kinetic energy coefficients, F and F', are the average of the two experimental geometry values (i.e., F = 5.7255 cm^{-1} and F' = –0.2036 cm^{-1} for acetone-h_6; F = 2.9955 cm^{-1} and F' = –0.1930 cm^{-1} for

Table VII. Comparison of Potential Constants and Torsional Fundamental Frequencies in Acetone-h_6 and -d_6[a]

method	V_3	V_{33}	V'_{33}	V_6	V_{eff}
empirical	370	136	−156	0	234
fully-relaxed HF/6-31G(d,p)	382.0	135.1	−171.3	−0.5	246.9
scaled MP2/6-31G(d,p)[b]	349.2	114.2	−141.8	−0.4	235.0
Crighton-Bell[c]	453	174	−167	0	279
Groner et al.[d]					
-h_6	279.4	−11.7	−108.2		291.1
-d_6	330	39	−108		291
Nelson-Pierce[e]					272

	acetone-h_6		acetone-d_6	
	$\nu_{12}(a_2)$	$\nu_{17}(b_2)$	$\nu_{12}(a_2)$	$\nu_{17}(b_2)$
experimental	77 ± 2	124.5 ± 0.1	55 ± 2	96.0 ± 0.1
empirical	77.9 ± 0.8	123.2 ± 1.8	54.2	94.9 ± 0.1
fully-relaxed HF/6-31G(d,p)	78.7 ± 0.7	128.3 ± 1.7	54.7	99.0 ± 0.1
scaled MP2/6-31G(d,p)[b]	78.9 ± 0.8	121.1 ± 1.8	55.5	93.5 ± 0.1
Crighton-Bell[f]	87.8 ± 0.5	134.7 ± 1.0	61.5	102.9
Groner et al.[g]	89.5 ± 0.6	124.2 ± 1.1	66.7	96.9
Nelson-Pierce[h]	101.6 ± 1.0	105.5 ± 1.0	75.6	80.8

[a] Potential constants and frequencies are in cm^{-1}. Predicted frequencies are averages of torsional sublevel energies with half-maximum splittings as their band half-widths (indicated if ≥0.1 cm^{-1}). [b] Scaling factor is 0.88. [c] Reference 7. [d] Reference 10. [e] Reference 4. [f] Torsional energies are computed with ref 7 potential constants and MW & GED kinetic energy coefficients in Table I. [g] Torsional energies are computed with ref 10 potential constants and MW kinetic energy coefficients in Table I. [h] Torsional energies are computed with ref 4 potential constant and MW kinetic energy coefficients in Table I.

Table VIII. Comparison of Experimental and Predicted Torsional Overtone Frequencies, $2\nu_{12}$, in Acetone-h_6 and -d_6[a]

method	acetone-h_6	acetone-d_6
experimental	162 ± 4	117 ± 2
empirical	164.9 ± 3.9	116.8 ± 0.3
scaled MP2/6-31G(d,p)	164.3 ± 4.1	117.6 ± 0.3
rigid-frame		
HF/DZ	206.7 ± 4.2	156.8 ± 0.2
HF/6-31G(d,p)	231.0 ± 2.8	174.2 ± 0.1
MP2/6-31G(d,p)	235.8 ± 2.5	178.1 ± 0.1
fully-relaxed		
HF/DZ	164.9 ± 3.5	114.8 ± 0.2
HF/6-31G(d,p)	167.7 ± 3.4	118.1 ± 0.2
MP2/6-31G(d,p)	176.1 ± 3.0	125.1 ± 0.2
Crighton-Bell[b]	185.2 ± 2.8	131.1 ± 0.1
Groner et al.[b]	175.4 ± 3.2	134.7 ± 0.2
Nelson-Pierce[b]	184.4 ± 6.6	145.4 ± 0.5

[a] Frequencies are in cm^{-1}. [b] See footnotes *f*–*h* in Table VII.

(28) The far-infrared 104.5-cm^{-1} band has been assigned to both $2\nu_{17} \leftarrow \nu_{17}$ and $\nu_{12} + \nu_{17} \leftarrow \nu_{12}$ transitions (see Table I, ref 10). These assignments based on torsional analysis do not take into account possible Fermi interactions.

(29) Though not reported in ref 2 higher sensitivity scans reveal the 12_2^1 band at –92 ± 2 cm^{-1} from the $3p_x \leftarrow$ n Rydberg origin in acetone-h_6, fixing $2\nu_{12}$" at 162 ± 4 cm^{-1}.

(30) Pulay, P.; Fogarasi, G.; Boggs, J. E. *J. Chem. Phys.* **1981**, *74*, 3999.

acetone-d_6). The three potential constants were varied to attain a 1-cm^{-1} agreement between predicted and experimental frequencies. The potential constants are V_3 = 370 cm^{-1}, V_{33} = 136 cm^{-1}, and V'_{33} = −156 cm^{-1} with 7 and 3 cm^{-1} estimated dispersions for $V_3 - V_{33}$ (V_{eff}) and V'_{33}, respectively. The three empirical potential constants are in qualitative agreement with the theoretical and scaled fully-relaxed model potential constants (Tables III and VII); they are within 10–15 cm^{-1} of the HF/6-31G(d,p) ones. The important outcome is that the empirical torsional potential function, although containing neither rigid-frame nor fully-relaxed concepts, agrees *only with the functions obtained from the fully-relaxed model.*

In summary, the close agreement between the fully-relaxed ab initio, scaled fully-relaxed ab initio, and empirical potential surfaces strongly supports flexing of the acetone skeleton occurring during the methyl rotations. The torsional Hamiltonian, eq 1, does not explicitly take into account interactions between the torsions and other vibrations. However, the geometry changes among the conformers (i.e., CCC and CCH bond angles and CC bond distances) inherent in the fully-relaxed model to a degree encompass the effect of these interactions into the torsional potential surface. The absence of these interactions (i.e., steric hinderance generated by methyl rotation) in the rigid-frame model is the reason for its poor predictive capabilities in acetone.

The barrier to torsional rotation $V_{eff} = V_3 - V_{33}$ is of chemical interest since it relates to entropy and heat capacity. The fully-relaxed model HF/6-31G(d,p) and scaled MP2/6-31G(d,p) potentials are in the vicinity of 240 cm^{-1} (Table VII). Wiberg and Martin[15] have calculated the barrier by ab initio methods HF through MP3 at the 6-31G(d) level and predict close to 300 cm^{-1}. The empirical potential barrier of 234 cm^{-1} (Table VII) instead agrees closely with the HF/6-31G(d,p) and scaled MP2/6-31G(d,p) values. It appears that the disparity between 6-31G(d) and 6-31G(d,p) barriers results from a difference in the CCC angle (2°) for the eclipsed–staggered geometry. The 240-cm^{-1} barrier deduced from torsional potential analysis represents a significant lowering from the 270-cm^{-1} Nelson-Pierce value obtained from microwave studies.[4]

There are large differences between the rigid-frame HF/DZ potential constants obtained in this study and the ones obtained by Crighton and Bell.[7] Although they used the rigid-frame model to generate the conformer energies, their optimized eclipsed–eclipsed conformer geometry was further restricted to equivalent hydrogens (i.e., bond lengths C–H_{ip} = C–H_{op} and bond angles H_{ip}–C–H_{op} = H_{op}–C–H_{op}). The optimized single C–H bond length, 1.0811 Å, in the Crighton–Bell calculation is 0.004 Å shorter than C–H_{op} in our calculation. This short CH bond calculation leads to ~100 cm^{-1} lower energies, e.g., for the 0°–30° and 30°–30° conformers, and thus underestimates the methyl–methyl interaction. The large differences between the Crighton–Bell and empirical potential constants (i.e., 83 cm^{-1} for V_3 and 38 cm^{-1} V_{33}) result in an ~10 cm^{-1} difference in fundamental frequencies (Table VII), and 15–20 cm^{-1} in the overtones (Table VIII).

The Groner et al.[10] empirical approach to obtaining potential surfaces from fine structure measurements in acetone-h_6, -d_6, and -d_3 fails to generate a unique potential. The potential constants are drastically different from the constants that we have discussed (i.e., the differences exceed 100 cm^{-1} for V_{33}) at any calculation level or assumed model. The unique V_{eff} and V'_{33} terms obtained from the Groner et al. analysis are 50 cm^{-1} higher than our empirical values. The outcome is a_2 fundamental frequencies ~12 cm^{-1} too high for acetone-h_6 and -d_6.

Another rigid-frame model torsional potential study was carried out by Smeyers and co-workers[11] using methods ranging from CNDO/2 to MP2(Frozen-Core)/6-31G(d,p) levels. These calculations were also restricted by equivalent hydrogens, but unlike the optimized Crighton–Bell geometry[7] they made use of a geometry (e.g., CC bond length 1.54 Å and CCC bond angle 120°) that is far from those obtained by experimental or theoretical methods. A six-term potential was employed of which the two additional terms beyond eq 3 were found to be negligible in the HF/6-31G calculation.

Table IX. Acetone HF/6-31G(d,p) Optimized Geometry Parameters for Methyl Conformers[a]

	τ_1–τ_2					
	60–60	60–0	0–0	60–30	30–0	30–30
	Bond Lengths					
C_1=O	1.1923	1.1924	1.1928	1.1922	1.1927	1.1924
C_1–C_2	1.5130	1.5104	1.5172	1.5116	1.5174	1.5136
C_1–C_3	1.5130	1.5173	1.5172	1.5151	1.5138	1.5136
C_2–H_1	1.0810	1.0810	1.0823	1.0810	1.0826	1.0873
C_2–H_2	1.0863	1.0867	1.0845	1.0862	1.0845	1.0841
C_2–H_3	1.0863	1.0867	1.0845	1.0868	1.0846	1.0820
C_3–H_4	1.0810	1.0832	1.0823	1.0871	1.0876	1.0873
C_3–H_5	1.0863	1.0845	1.0845	1.0839	1.0835	1.0841
C_3–H_6	1.0863	1.0845	1.0845	1.0819	1.0820	1.0820
	Bond Angles					
C_2–C_1=O	121.65	121.87	120.22	121.76	120.40	121.25
C_3–C_1=O	121.65	120.59	120.22	121.14	121.02	121.25
C_2–C_1–C_3	116.70	117.54	119.56	117.10	118.58	117.51
C_1–C_2–H_1	109.74	109.92	113.33	109.86	113.24	108.50
C_1–C_2–H_2	110.29	110.08	108.74	110.01	109.05	112.35
C_1–C_2–H_3	110.29	110.08	108.74	110.28	108.58	109.53
C_1–C_3–H_4	109.74	113.00	113.33	108.83	108.60	108.50
C_1–C_3–H_5	110.29	108.88	108.74	112.25	112.47	112.35
C_1–C_3–H_6	110.29	108.88	108.74	109.49	109.35	109.53
H_1–C_2–H_2	109.63	109.79	109.24	109.61	109.26	108.20
H_2–C_2–H_3	107.23	107.13	107.37	107.25	107.48	110.25
H_4–C_3–H_5	109.63	109.21	109.24	107.90	108.19	108.20
H_5–C_3–H_6	107.23	107.51	107.37	108.03	110.29	110.25

[a] Bond lengths and bond angles are in Å and deg, respectively. Molecular frames (i.e., oxygen and three carbons) are always held in a plane. Atom numbering is shown in Figure 1a. Torsional angles, τ_1 and τ_2, defining conformers, refer to H_1 and H_4, respectively.

5. Conclusions

Rigid-frame torsional potential surfaces generated by ab initio calculations do not realize the large-amplitude vibrations in acetone with reasonable accuracy. In contrast, the fully-relaxed model allowing skeletal flexibility during methyl rotations produces a potential surface, which gives impressive agreement between experimental and predicted torsional frequencies.

The predictive capability of the fully relaxed model should be exploitable by high-resolution infrared jet experiments involving sublevel splittings of the b_2 torsional fundamental.

The potential terms obtained from the fully-relaxed model are in very close agreement with terms empirically derived from measured fundamental and overtone frequencies. We conclude that the fully-relaxed model represents a more physical approach to the torsional potential surface problem. An important outcome of this model is significant lowering of the torsional potential barrier to 240 cm^{-1} from the microwave 270-cm^{-1} value.

The utility of Rydberg spectroscopy in developing a torsional barrier potential model has been demonstrated. Secure ground-state a_2 torsional vibration frequency information allows strong discrimination between the rigid-frame and fully-relaxed models and construction of a unique ground-state empirical torsional potential.

In forthcoming papers we extend the ideas discussed here and in the preceding article[2] to other two methyl top molecules including dimethyl ether and thioacetone.

Acknowledgment. We are grateful to Rutgers University for a Research Council grant and a Supercomputer Postdoctoral Fellowship for A.G.O. We thank Stephen Bell for helpful correspondence. We are especially grateful to Dr. Peter Groner for his valuable comments on the manuscript. The calculations were carried out at the Pittsburgh Supercomputer Center via a grant from this center.

Appendix

Acetone HF/6-31G(d,p) optimized geometry parameters for the six methyl conformers are given in Table IX. All possible geometry parameters are optimized with the exception that oxygen and three carbons are held in a plane. The conformers are defined by the torsional angles of one hydrogen on each methyl group.